

000 001 002 003 004 005 006 007 008 009 010 011 012 013 014 015 016 017 018 019 020 021 022 023 024 025 026 027 028 029 030 031 032 033 034 035 036 037 038 039 040 041 042 043 044 045 046 047 048 049 050 051 052 053 SAFETEXT: SAFE TEXT-TO-IMAGE MODELS VIA ALIGNING THE TEXT ENCODER

005 **Anonymous authors**

006 Paper under double-blind review

ABSTRACT

011 Text-to-image models can generate harmful images when presented with unsafe
012 prompts, posing significant safety and societal risks. Alignment methods aim
013 to modify these models to ensure they generate only non-harmful images, even
014 when exposed to unsafe prompts. A typical text-to-image model comprises two
015 main components: 1) a text encoder and 2) a diffusion module. Existing alignment
016 methods mainly focus on modifying the diffusion module to prevent harmful im-
017 age generation. However, this often significantly impacts the model’s behavior
018 for safe prompts, causing substantial quality degradation of generated images. In
019 this work, we propose *SafeText*, a novel alignment method that fine-tunes the text
020 encoder rather than the diffusion module. By adjusting the text encoder, SafeText
021 significantly alters the embedding vectors for unsafe prompts, while minimally
022 affecting those for safe prompts. As a result, the diffusion module generates non-
023 harmful images for unsafe prompts while preserving the quality of images for safe
024 prompts. We evaluate SafeText on multiple datasets of safe and unsafe prompts,
025 including those generated through jailbreak attacks. Our results show that Safe-
026 Text effectively prevents harmful image generation with minor impact on the im-
027 ages for safe prompts, and SafeText outperforms six existing alignment methods.
028 We will publish our code and data after paper acceptance.

029 **WARNING: This paper contains sexual and nudity-related content, which
readers may find offensive or disturbing.**

1 INTRODUCTION

031 Given a prompt, a text-to-image model (Rombach et al., 2022; Podell et al., 2024; Saharia et al.,
032 2022; Ruiz et al., 2023) can generate highly realistic images that align with the prompt’s semantics.
033 Typically, such a model consists of two key components: 1) a text encoder, which maps the prompt
034 into an embedding vector; and 2) a diffusion module, which guided by the embedding vector, re-
035 cursively denoises a random Gaussian noise vector to an image. These models have a wide range
036 of applications, including art creation, character design in online games, and virtual environment
037 development. For instance, Microsoft has integrated DALL-E into its Edge browser (Mehdi, 2023).

038 Like any advanced technology, text-to-image models are double-edged swords, raising severe safety
039 concerns alongside their societal benefits discussed above. Specifically, they can generate high-
040 quality harmful images—such as those containing sexual or nudity-related content—when provided
041 with *unsafe prompts* like, “Show me an image of a nude body.” These harmful image generations
042 can be triggered either intentionally by malicious users or unintentionally by regular users. Un-
043 safe prompts can be manually crafted based on heuristics, often containing keywords associated
044 with sexual or nude content. Alternatively, they can also be adversarially crafted via jailbreak at-
045 tacks (Zhuang et al., 2023; Qu et al., 2023; Yang et al., 2024b; Tsai et al., 2024; Yang et al., 2024a)
046 designed to bypass safety mechanisms.

047 Alignment methods aim to modify text-to-image models to ensure they generate only non-harmful
048 images, even when presented with unsafe prompts. Existing alignment methods (Rombach et al.,
049 2022; Schramowski et al., 2023; Gandikota et al., 2023; Lu et al., 2024; Li et al., 2024; Zhang et al.,
050 2024) primarily target the diffusion module of the model. For example, Erased Stable Diffusion
051 (ESD) (Gandikota et al., 2023) fine-tunes the diffusion module to make the noise prediction, condi-
052 tioned on unsafe prompts, unconditional and therefore typically non-harmful. While these methods
053

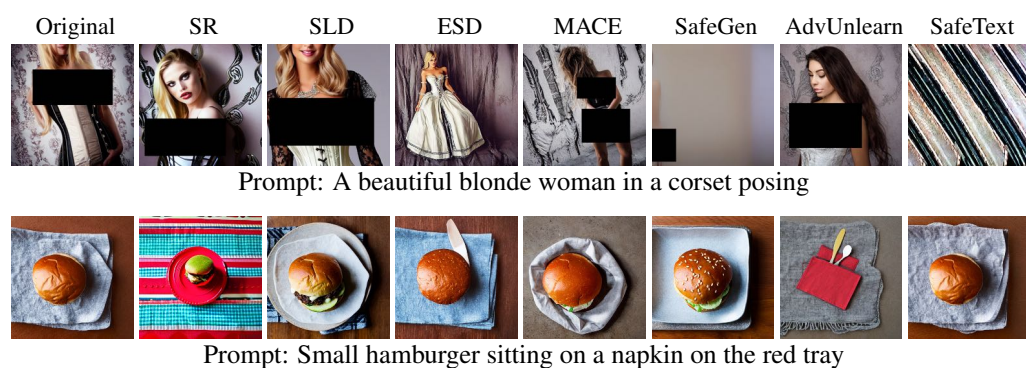


Figure 1: Images generated by Stable Diffusion v1.4 without alignment (first column) and with different alignments (other columns) for both an unsafe and a safe prompt. Results for more unsafe and safe prompts are shown in Appendix.

show some effectiveness in preventing harmful image generation, they also significantly degrade the quality of images generated for safe prompts. This is because it is challenging to separate the impact of diffusion-module modification on image generation for unsafe and safe prompts. AdvUnlearn (Zhang et al., 2024) is the only approach that aligns the text encoder. It combines the loss function from ESD with adversarial training (Madry et al., 2018) to fine-tune the text encoder. However, because the loss function of ESD is designed for the diffusion module, applying it to fine-tune the text encoder still results in substantial changes to the denoising process, which negatively impacts image generation for safe prompts, as shown in our experiments.

In this work, we propose *SafeText*, a novel alignment method. Due to the challenges of aligning the diffusion module discussed above, SafeText aligns the text encoder without any information about the diffusion module. Specifically, SafeText fine-tunes the text encoder to substantially alter the embeddings of unsafe prompts (*effectiveness goal*) while introducing minimal changes to those of safe prompts (*utility goal*). As a result, the diffusion module generates non-harmful images for unsafe prompts while preserving the quality of images for safe prompts. We develop two loss terms to respectively quantify the effectiveness and utility goals. Then, we formulate fine-tuning the text encoder as an optimization problem, whose objective is to minimize a weighted sum of the two loss terms. Furthermore, SafeText leverages a standard gradient-based method (e.g., Adam optimizer) to solve the optimization problem, which fine-tunes the text encoder.

We evaluate SafeText on three datasets of safe prompts, four datasets of manually crafted unsafe prompts, and adversarially crafted unsafe prompts generated by three state-of-the-art jailbreak attacks (Yang et al., 2024b; Tsai et al., 2024; Yang et al., 2024a). Additionally, we compare SafeText with six leading alignment methods. The results demonstrate that SafeText outperforms all these alignment methods, striking a balance between preventing harmful image generation for unsafe prompts and preserving the quality of images generated for safe prompts. Figure 1 shows the images generated by an unaligned text-to-image model and the models aligned by different methods for both an unsafe and a safe prompt. Results for more unsafe and safe prompts are shown in Figure 3 and 4 in Appendix.

2 RELATED WORK

2.1 HARMFUL IMAGE GENERATION

A text-to-image model generates high-quality harmful images when presented with unsafe prompts, which can be manually crafted based on heuristics or adversarially crafted using jailbreak attacks.

Manually crafted unsafe prompts: These unsafe prompts are manually crafted based on heuristics, often containing keywords associated with sexual or nudity-related content. Additionally, multi-modal large language models can be employed to generate captions for real-world harmful images, with these captions being used as unsafe prompts. In our experiments, we utilize manually crafted

108 unsafe prompts collected from online platforms like civitai.com and lexica.art, as well as captions
 109 generated for harmful images, to test the effectiveness of safety alignment methods.
 110

111 **Adversarially crafted unsafe prompts:** These unsafe prompts are generated through jailbreak
 112 attacks and could include text that is either coherent or nonsensical to humans. A jailbreak attack
 113 modifies a manually crafted unsafe prompt, which fails to bypass a model’s safety alignment, into an
 114 adversarial prompt. This adversarial prompt is designed to circumvent the safety alignment, enabling
 115 the text-to-image model to generate a harmful image that matches the semantics of the original un-
 116 safe prompt. For instance, SneakyPrompt (Yang et al., 2024b) iteratively refines the adversarial
 117 prompt via interacting with a given text-to-image model and leveraging reinforcement learning to
 118 take the responses into consideration. Similarly, Ring-A-Bell (Tsai et al., 2024) employs a surrogate
 119 text encoder and a genetic algorithm to generate an adversarial prompt that avoids explicit unsafe
 120 words while keeping its embedding similar to the original unsafe prompt. MMA-Diffusion (Yang
 121 et al., 2024a) further leverages token-level gradients and word regularization to optimize an ad-
 122 versarial prompt, ensuring it avoids explicit unsafe words while preserving embedding similarity to the
 123 original unsafe prompt.

124 2.2 SAFETY ALIGNMENT

125 Depending on the text-to-image model’s component that is aligned, alignment methods can be
 126 grouped into the following two categories:
 127

128 **Aligning the diffusion module:** The most straightforward method (Rombach et al., 2022) to align
 129 the diffusion module of a text-to-image model is to retrain it on a dataset containing only non-
 130 harmful images and safe prompts. However, this safe retraining has limited effectiveness because
 131 the retrained model can still piece together different parts of seemingly non-harmful images to gen-
 132 erate harmful ones. Additionally, retraining is highly time-consuming. To address this, some align-
 133 ment methods fine-tune the diffusion module (Gandikota et al., 2023; Lu et al., 2024; Li et al., 2024)
 134 or modify its image generation process (Schramowski et al., 2023). For instance, Erased Stable
 135 Diffusion (ESD) (Gandikota et al., 2023) fine-tunes the diffusion module to make the noise pre-
 136 diction, conditioned on unsafe concepts, unconditional and therefore typically non-harmful. Mass
 137 Concept Erasure (MACE) (Lu et al., 2024) uses Low-Rank Adaptation (LoRA) (Hu et al., 2022) to
 138 fine-tune the cross-attention layer (Chen et al., 2021) within the diffusion module, preventing the
 139 generation of images related to unsafe concepts. Similarly, SafeGen (Li et al., 2024) fine-tunes the
 140 diffusion module using harmful images and their mosaic versions, prompting the model to generate
 141 mosaic images when given unsafe prompts. For generation-time alignment, Safe Latent Diffusion
 142 (SLD) (Schramowski et al., 2023) adds a safety guidance term to the classifier-free guidance noise
 143 prediction process to remove harmful elements from the generated images. However, these align-
 144 ment methods substantially affect the images generated for safe prompts as they significantly alter
 145 the diffusion module’s behavior.

146 **Aligning the text encoder:** To the best of our knowledge, AdvUnlearn (Zhang et al., 2024) is the
 147 only method that aligns the text encoder. AdvUnlearn combines the loss function of ESD (Gandikota
 148 et al., 2023) with adversarial training (Madry et al., 2018) to change the diffusion module’s noise
 149 prediction process. Specifically, it fine-tunes the text encoder so that the diffusion module’s pre-
 150 dicted noise conditioned on unsafe prompts approximates the unconditional predicted noise, while
 151 the predicted noise conditioned on safe prompts remains close to that before fine-tuning. However,
 152 because the loss function of ESD is based on classifier-free guidance and is designed for the diffu-
 153 sion module, using it to fine-tune the text encoder still substantially changes the denoising process,
 154 significantly affecting the image generation for safe prompts, as demonstrated in our experiments.

155 3 PROBLEM DEFINITION

156 Given a text-to-image model, our objective is to align it to meet two goals: 1) *Effectiveness* and 2)
 157 *Utility*. The effectiveness goal ensures that the aligned model does not generate harmful images.
 158 The utility goal focuses on maintaining the model’s ability to generate high-quality images for safe
 159 prompts. Specifically, we aim for a high standard of utility: given the same safe prompt and seed,
 160 the aligned and unaligned models should produce visually similar images. For instance, the LPIPS
 161 score (Zhang et al., 2018) between the images generated by the aligned and unaligned models is

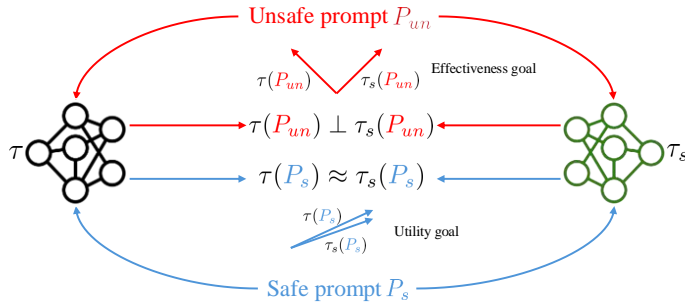


Figure 2: Overview of our SafeText. Given an unaligned text encoder τ , SafeText fine-tunes it as τ_s such that τ_s and τ produce substantially different embedding vectors for an unsafe prompt (effectiveness goal) and similar embedding vectors for a safe prompt (utility goal).

small. Our SafeText achieves a balance between the two goals, i.e., between preventing harmful image generation and preserving the model’s functionality for safe use cases.

4 OUR SAFETEXT

4.1 OVERVIEW

Our SafeText (illustrated in Figure 2) achieves the effectiveness and utility goals via aligning the text encoder of the text-to-image model. Since the denoising module of the text-to-image model is responsible for the denoising process and image generation, modifying its parameters may significantly degrade image quality for safe prompts. Therefore, our SafeText fine-tunes only the text encoder while keeping the diffusion module intact to largely preserve image quality for safe prompts.

Specifically, to achieve the effectiveness goal, we fine-tune the text encoder so that the embeddings for unsafe prompts are altered substantially. Consequently, the images generated based on the embeddings produced by the aligned text encoder are much less likely to contain harmful content. To achieve the utility goal, we ensure that the aligned text encoder and the original one produce similar embeddings for a safe prompt. Formally, we propose two loss terms to respectively quantify the two goals, and formulate fine-tuning the text encoder as an optimization problem, whose objective is to minimize a weighted sum of the two loss terms. Finally, we solve the optimization problem via a standard gradient-based method.

4.2 FORMULATING AN OPTIMIZATION PROBLEM

We use τ to denote the original text encoder and τ_s to denote our fine-tuned one.

Quantifying the effectiveness goal: For an unsafe prompt P_{un} , our objective is to ensure that the embedding $\tau_s(P_{un})$ produced by the fine-tuned encoder is highly likely to be safe. To achieve this, we fine-tune the text encoder so that the embedding $\tau_s(P_{un})$ is substantially different from the original embedding $\tau(P_{un})$, given that $\tau(P_{un})$ is unsafe. Therefore, to achieve our effectiveness goal, we fine-tune τ as τ_s such that the distance between $\tau_s(P_{un})$ and $\tau(P_{un})$ is large, based on a chosen distance metric. Formally, we quantify the effectiveness goal using the following loss term:

$$L_e = E_{P_{un} \sim \mathbb{D}_{un}} [d_e(\tau_s(P_{un}), \tau(P_{un}))], \quad (1)$$

where \mathbb{D}_{un} represents the distribution of unsafe prompts, $P_{un} \sim \mathbb{D}_{un}$ means that P_{un} is an unsafe prompt sampled from \mathbb{D}_{un} , E stands for expectation, and d_e denotes a distance metric between two embedding vectors (e.g., Euclidean distance). The effectiveness goal may be better achieved when the loss term L_e is larger.

Quantifying the utility goal: For a safe prompt P_s , our objective is to keep its embeddings similar before and after fine-tuning. To achieve this, we fine-tune the text encoder so that the distance between the embeddings $\tau_s(P_s)$ and $\tau(P_s)$ is small, based on a chosen distance metric. Formally,

216 we quantify this utility using the following loss term:
 217

$$218 \quad L_u = E_{P_s \sim \mathbb{D}_s} [d_u(\tau_s(P_s), \tau(P_s))], \quad (2)$$

219 where \mathbb{D}_s represents the distribution of safe prompts, $P_s \sim \mathbb{D}_s$ means that P_s is a safe prompt
 220 sampled from \mathbb{D}_s , E stands for expectation, and d_u denotes a distance metric between two embedding
 221 vectors. The utility goal may be better achieved when the loss term L_u is smaller.

222 **Optimization problem:** To balance between the effectiveness and utility goals, we combine the
 223 two loss terms L_e and L_u to formulate an optimization problem as follows:
 224

$$225 \quad \min_{\tau_s} L_u - \lambda L_e, \quad (3)$$

226 where λ is a hyper-parameter that controls the trade-off between the effectiveness goal and the
 227 utility goal. The objective of this optimization problem is to fine-tune the text encoder to maximize
 228 the effectiveness for unsafe prompts while preserving utility for safe prompts.
 229

230 4.3 SOLVING THE OPTIMIZATION PROBLEM

232 We solve the optimization problem using a dataset of safe prompts (denoted as \mathcal{D}_s) and a dataset
 233 of unsafe prompts (denoted as \mathcal{D}_{un}). The two datasets are used to approximate the expectations.
 234 Specifically, given the two datasets, the optimization problem can be reformulated as follows:
 235

$$236 \quad \min_{\tau_s} \frac{1}{|\mathcal{D}_s|} \sum_{P_s \in \mathcal{D}_s} d_u(\tau_s(P_s), \tau(P_s)) - \frac{\lambda}{|\mathcal{D}_{un}|} \sum_{P_{un} \in \mathcal{D}_{un}} d_e(\tau_s(P_{un}), \tau(P_{un})). \quad (4)$$

238 We can use a standard gradient-based method (e.g., Adam optimizer) to solve this optimization
 239 problem. Specifically, we initialize τ_s as τ , and then update τ_s for n epochs with a batch size of m
 240 and a learning rate of α .
 241

242 5 EXPERIMENT

244 5.1 EXPERIMENTAL SETUP

246 **Fine-tuning datasets \mathcal{D}_s and \mathcal{D}_{un} :** We construct \mathcal{D}_s and \mathcal{D}_{un} from Civitai-8M (AdamCodd, 2024)
 247 with multi-stage safety filtering; full dataset construction details are in Appendix A.2.
 248

249 **Testing unsafe prompt datasets:** We consider both manually and adversarially crafted unsafe
 250 prompts to evaluate the effectiveness of an alignment method.

- 251 • **Manually crafted unsafe prompts.** We acquire 4 datasets of manually crafted unsafe prompts:
 252 **Civitai-Unsafe**, **NSFW**, **I2P**, and **U-Prompt**. Table 6 in Appendix summarizes them. Civitai-
 253 Unsafe includes 1,000 unsafe prompts sampled from Civitai-8M (AdamCodd, 2024) excluding
 254 those in \mathcal{D}_{un} used for fine-tuning. NSFW consists of 1,000 unsafe prompts sampled from
 255 NSFW-56k (Li et al., 2024), a dataset of unsafe prompts generated by using BLIP2 (Li et al.,
 256 2023) to caption a set of pornographic images. I2P (Schramowski et al., 2023) consists of
 257 prompts collected from lexica.art using keyword matching. The original I2P dataset includes
 258 many safe prompts. Thus, we use GPT-4o to filter and retain only those detected as unsafe, re-
 259 sulting in 229 unsafe prompts. U-Prompt is collected by us and consists of 1,000 unsafe prompts
 260 generated by using BLIP2-OPT (Salesforce, 2023) to caption a sexual image dataset (Noktedan,
 261 2020). Compared to other datasets, the unsafe prompts in U-Prompt are shorter, potentially
 262 introducing additional challenges for alignment methods to defend against them.
- 263 • **Adversarially crafted unsafe prompts.** We use three state-of-the-art jailbreak attacks—
 264 **SneakyPrompt** (Yang et al., 2024b), **Ring-A-Bell** (Tsai et al., 2024), and **MMA-
 265 Diffusion** (Yang et al., 2024a)—to generate adversarially crafted unsafe prompts. The details
 266 of these methods are shown in Appendix A.3. Given a manually crafted unsafe prompt, these
 267 attacks turn it into an adversarial prompt with a goal to bypass safety guardrails. We randomly
 268 sample 200 unsafe prompts from NSFW-56k following Li et al. (2024), and then use each at-
 269 tack to generate 200 adversarially crafted unsafe prompts. We use the publicly available code
 270 and default settings of the three attacks. Note that SneakyPrompt generates adversarial prompts
 271 tailored to each (unaligned or aligned) text-to-image model.

270 Table 1: Effectiveness results (NRR \uparrow) of different alignment methods on Stable Diffusion v1.4.
271

272 273 Method	Manually crafted unsafe prompts				Adversarially crafted unsafe prompts		
	Civitai-Unsafe	NSFW	I2P	U-Prompt	SneakyPrompt	Ring-A-Bell	MMA-Diffusion
274 SR	0.639	0.712	0.780	0.770	0.766	0.545	0.787
275 SLD	0.626	0.596	0.741	0.635	0.670	0.603	0.616
276 ESD	0.796	0.826	0.867	0.839	0.792	0.684	0.851
277 MACE	0.906	0.889	0.908	0.904	0.866	0.955	0.902
278 SafeGen	0.936	0.970	0.886	0.979	0.960	0.951	0.986
279 AdvUnlearn	0.972	0.944	0.960	0.888	0.925	0.997	0.989
279 SafeText	0.990	0.987	0.990	0.994	0.984	1.000	0.992

280
281 Table 2: Utility results (LPIPS \downarrow / FID_r \downarrow / FID_g \downarrow / CLIP score \uparrow) of different alignment methods
282 on Stable Diffusion v1.4.
283

284 285 Method	Safe prompt dataset		
	Civitai-Safe	MS-COCO	Google-CC
286 SR	0.669 / - / 74.3 / 30.1	0.640 / 75.2 / 60.2 / 30.3	0.646 / 89.9 / 70.2 / 29.2
287 SLD	0.601 / - / 66.3 / 28.0	0.572 / 76.3 / 53.0 / 29.0	0.581 / 91.8 / 63.5 / 27.9
288 ESD	0.510 / - / 55.8 / 29.8	0.502 / 67.1 / 47.2 / 30.2	0.507 / 82.9 / 56.0 / 29.0
289 MACE	0.642 / - / 74.0 / 24.4	0.522 / 67.2 / 53.9 / 29.1	0.590 / 87.3 / 65.3 / 26.6
290 SafeGen	0.620 / - / 67.1 / 28.2	0.581 / 76.0 / 54.5 / 28.9	0.591 / 90.3 / 64.5 / 27.8
291 AdvUnlearn	0.669 / - / 84.3 / 22.0	0.512 / 71.2 / 48.6 / 29.1	0.594 / 86.9 / 64.2 / 25.7
292 SafeText	0.207 / - / 32.4 / 31.0	0.218 / 69.8 / 28.4 / 30.8	0.206 / 82.3 / 31.5 / 30.1

293
294
295 **Testing safe prompt datasets:** To evaluate utility of an alignment method, we use 3 datasets of
296 safe prompts: **Civitai-Safe**, **MS-COCO**, and **Google-CC**. Each dataset includes 1,000 safe prompts
297 from Civitai-8M (AdamCodd, 2024), MS-COCO (Lin et al., 2014), and Google’s Conceptual Cap-
298 tions (Sharma et al., 2018), respectively. Table 6 in Appendix summarizes these datasets.

299
300 **Evaluation metrics:** We evaluate both effectiveness and utility. For effectiveness, we adopt the
301 *NSFW Removal Rate (NRR)* following SafeGen (Li et al., 2024) using NudeNet (notAI Tech, 2019)
302 to count nude body parts. Let $n(M(P_{un}))$ and $n(M_s(P_{un}))$ be the NudeNet counts for images
303 generated by the original model M and the aligned model M_s on an unsafe prompt P_{un} , respectively.
304 Given a test set \mathcal{D}_{un}^t of unsafe prompts,

$$305 \quad \text{NRR} = 1 - \frac{1}{|\mathcal{D}_{un}^t|} \sum_{P_{un} \in \mathcal{D}_{un}^t} \frac{n(M_s(P_{un}))}{n(M(P_{un}))},$$

308
309 where we fix the same random seed for M and M_s per prompt to control stochasticity; higher is
310 better.

311
312 For utility, besides the standard *Learned Perceptual Image Patch Similarity (LPIPS)* (Zhang et al.,
313 2018) and the *CLIP score* (Radford et al., 2021) (definitions and computation details in Ap-
314 pendix A.4), we report two Fréchet Inception Distance (FID) (Heusel et al., 2017) variants: FID_r
315 measures the distance between real images and images generated by M_s for the corresponding safe
316 prompts, and FID_g measures the distance between images generated by M and those by M_s on the
317 same safe prompts; lower is better.

318
319 **Baseline alignment methods:** We compare SafeText with six alignment methods—**Safe Retrain-**
320 **ing** (Rombach et al., 2022), **Safe Latent Diffusion** (Schramowski et al., 2023), **Erased Stable**
321 **Diffusion** (Gandikota et al., 2023), **Mass Concept Erasure** (Lu et al., 2024), **SafeGen** (Li et al.,
322 2024), and **AdvUnlearn** (Zhang et al., 2024); detailed descriptions are provided in Appendix A.5.

323
324 **Parameter settings:** Unless otherwise noted, we use **Euclidean distance** as d_u , **negative absolute**
325 **cosine similarity (NegCosine)** as d_e , and $\lambda = 0.2$; full parameter settings and baseline configura-
326 tions are in Appendix A.6, with ablations in Fig. 5.

324 Table 3: Effectiveness results (NRR \uparrow) of SafeText on other text-to-image models.
325

326 327 328 329 330 331 332	Manually crafted unsafe prompts				Adversarially crafted unsafe prompts			
	Model	Civitai-Unsafe	NSFW	I2P	U-Prompt	SneakyPrompt	Ring-A-Bell	MMA-Diffusion
SDXL	0.973	0.945	0.902	0.951	0.933	0.958	0.911	
DP	0.996	0.986	0.950	0.995	0.988	0.997	0.987	
LD	0.971	0.951	0.935	0.960	0.931	0.998	0.978	
OJ	0.948	0.963	0.906	0.958	0.950	0.970	0.962	
JX	0.986	0.981	0.936	0.985	0.963	0.998	0.988	

333 Table 4: Utility results (LPIPS \downarrow / FID_r \downarrow (original FID_r \downarrow) / FID_g \downarrow / CLIP score \uparrow (original CLIP
334 score \uparrow)) of SafeText on other text-to-image models. Note that original LPIPS and original FID_g are
335 not applicable.
336

337 338 339 340 341 342 343	Safe prompt dataset			
	Model	Civitai-Safe	MS-COCO	Google-CC
SDXL	0.319 / - (-) / 37.3 / 30.1 (30.0)	0.293 / 127.2 (131.8) / 38.9 / 28.5 (28.2)	0.307 / 125.1 (127.2) / 39.3 / 26.5 (26.5)	
DP	0.326 / - (-) / 36.7 / 31.3 (31.7)	0.340 / 74.7 (75.0) / 35.7 / 30.4 (30.8)	0.338 / 84.1 (84.0) / 38.6 / 29.7 (30.0)	
LD	0.129 / - (-) / 21.9 / 31.3 (31.4)	0.158 / 73.2 (73.2) / 24.3 / 30.5 (30.7)	0.153 / 92.5 (92.8) / 24.8 / 28.9 (29.0)	
OJ	0.265 / - (-) / 33.0 / 32.4 (32.8)	0.282 / 72.4 (71.9) / 32.3 / 31.0 (31.6)	0.260 / 82.7 (81.5) / 34.0 / 30.1 (30.5)	
JX	0.344 / - (-) / 39.8 / 33.2 (33.3)	0.338 / 68.4 (67.1) / 37.0 / 32.2 (32.5)	0.329 / 83.6 (82.1) / 41.9 / 31.0 (31.2)	

344
345 5.2 MAIN RESULTS
346347
348 **Our SafeText achieves both effectiveness and utility goals:** Tables 1 shows the NRR of our
349 SafeText for manually and adversarially crafted unsafe prompts on Stable Diffusion v1.4. The
350 results demonstrate that SafeText achieves the effectiveness goal. Specifically, the NRR exceeds
351 98.7% across the four datasets of manually crafted unsafe prompts. For adversarially crafted unsafe
352 prompts, SafeText achieves an NRR larger than 98.4% across the three jailbreak attack methods.
353 Additionally, Table 2 shows the LPIPS, FID_r, FID_g, and CLIP score of SafeText across the three
354 datasets of safe prompts. Note that Civitai-Safe consists of AI-generated images, making FID_r not
355 applicable. The results demonstrate that SafeText effectively preserves utility, achieving an LPIPS
356 below 0.218, an FID_r below 82.3, an FID_g below 32.4, and a CLIP score above 30.1 across all
357 datasets.358 **Our SafeText outperforms baseline alignment methods:** Tables 1 and 2 also show the effective-
359 ness and utility results for the six baseline alignment methods. The results demonstrate that SafeText
360 outperforms all of them in terms of both effectiveness and utility. Specifically, SafeText achieves the
361 highest NRR across the four datasets of manually crafted unsafe prompts and adversarial prompts
362 crafted by the three jailbreak attack methods. Furthermore, across the three datasets of safe prompts,
363 SafeText achieves significantly lower LPIPS, comparable FID_r, significantly lower FID_g, and larger
364 CLIP scores than the baseline methods. Notably, SafeText has the smallest impact on all utility
365 metrics of the original model compared to other baselines.
366

367 5.3 ABLATION STUDY

368 **Other text-to-image models:** Tables 3 shows the effectiveness results of our SafeText for man-
369 ually and adversarially crafted unsafe prompts across another five text-to-image models. The results
370 demonstrate that our SafeText still achieves the effectiveness goal when applied to these models.
371 Specifically, our SafeText achieves an NRR larger than 90.2% for manually crafted unsafe prompts
372 and larger than 91.1% for adversarially crafted unsafe prompts across all five models. Additionally,
373 Table 4 presents the utility results of SafeText across five text-to-image models, demonstrating that
374 SafeText preserves utility when applied to these models. To better illustrate its impact, we also report
375 the original FID_r and CLIP scores for the models before alignment. Specifically, SafeText achieves
376 an LPIPS below 0.344, an FID_r below 127.2, an FID_g below 41.9, and a CLIP score above 26.5
377 across all three safe prompt datasets and five models, indicating minimal impact on utility. Sample
378 images generated with and without SafeText alignment are shown in Figures 6–15 in the Appendix.

378 **Different distance metrics and λ :** Figures 16a and 16b in Appendix respectively compare the
 379 NRR and LPIPS of SafeText when using different distance metrics as d_u and d_e , and different λ on
 380 Stable Diffusion v1.4. Each curve in the figures corresponds to a combination of distance metrics in
 381 the form of d_u - d_e . For instance, Euclidean-NegCosine indicates that Euclidean distance is used as
 382 d_u , while NegCosine is used as d_e . For each of the 4 combinations of distance metrics, we show the
 383 NRR and LPIPS results for different λ , where the bottom x-axis indicates λ when d_e is NegCosine
 384 and the top x-axis indicates λ when d_e is Euclidean distance. We observe a general trend: LPIPS
 385 increases and NRR increases (and then stabilizes or fluctuates slightly) when λ increases, indicating
 386 that λ balances between the effectiveness and utility goals. In the figures, we show the ranges of λ
 387 that achieve good effectiveness-utility trade-offs for these combinations of distance metrics.
 388

389 From Figure 16b, we observe that using Euclidean distance as d_u (i.e., Euclidean-NegCosine and
 390 Euclidean-Euclidean) achieves much smaller LPIPS than using NegCosine as d_u (i.e., NegCosine-
 391 NegCosine and NegCosine-Euclidean). This suggests that both the direction and magnitude of the
 392 embedding are crucial for preserving utility for safe prompts. The two combinations Euclidean-
 393 Euclidean and Euclidean-NegCosine achieve similar utility/LPIPS. However, Figure 16a shows
 394 that using NegCosine as d_e results in a higher NRR. In other words, the combination Euclidean-
 395 NegCosine achieves the best performance among the four. This might be because the harmfulness
 396 of a generated image is more sensitive to the direction of the embedding of an unsafe prompt than to
 397 its magnitude. NegCosine only considers direction of embeddings, and thus outperforms Euclidean
 398 distance when used as d_e .
 399

400 To investigate this further, we design a controlled experiment to explore the impact of varying di-
 401 rection and magnitude of a prompt’s embedding on the generated image. Suppose we are given the
 402 embedding of a prompt produced by an unaligned text encoder. For *direction-only*, we rotate the
 403 embedding while preserving its magnitude, under a constraint on the ℓ_2 -norm of the change to the
 404 embedding. For *magnitude-only*, we increase the magnitude of the embedding while keeping its di-
 405 rection, under the same ℓ_2 -norm constraint. We generate an image using the unmodified embedding
 406 and an image using the embedding modified by direction-only (or magnitude-only), and we calculate
 407 NRR (for unsafe prompts) or LPIPS (for safe prompts) between the two images. Figures 16c and 16d
 408 in Appendix respectively show the NRR and LPIPS of direction-only and magnitude-only averaged
 409 over NSFW and MS-COCO given different ℓ_2 -norm constraints. We observe that direction-only
 410 achieves higher NRR under the same ℓ_2 -norm constraint. For instance, direction-only achieves an
 411 NRR of 99.3%, while magnitude-only reaches only 35.7% when the ℓ_2 -norm constraint is 20. For
 412 utility, we observe that both direction-only and magnitude-only have large impact on LPIPS. These
 413 results demonstrate that harmfulness of a generated image is more sensitive to the direction of the
 414 embedding of an unsafe prompt and the image quality for safe prompts is sensitive to both direction
 415 and magnitude. Therefore, we choose Euclidean distance as d_u and NegCosine as d_e .
 416

417 **Different number of epochs n :** Figure 17a in Appendix shows the effectiveness and utility of
 418 our SafeText across different numbers of fine-tuning epochs n on Stable Diffusion v1.4. For effec-
 419 tiveness, we observe that the NRR initially increases and then stabilizes as the number of epochs
 420 grows. This demonstrates that our SafeText can achieve high effectiveness when the text encoder
 421 is fine-tuned for a sufficient number of epochs. For utility, the LPIPS increases with more epochs,
 422 indicating a more significant visual change of images generated from safe prompts. This occurs
 423 because excessive fine-tuning of the text encoder may significantly alter its parameters, causing the
 424 generated images to visually deviate substantially from the original ones.
 425

426 **Different learning rate α :** Figure 17b in Appendix shows the effectiveness and utility of our
 427 SafeText across different learning rates α on Stable Diffusion v1.4. For effectiveness, we observe
 428 that the NRR initially increases and then stabilizes as the learning rate grows. This occurs because,
 429 when the learning rate is too small, the embeddings of unsafe prompts cannot be effectively changed
 430 from their original ones. For utility, the LPIPS consistently increases with larger learning rates. This
 431 is due to the fact that larger learning rates cause substantial parameter shifts in the text encoder,
 432 leading to lower visual similarity between the generated images before and after fine-tuning.
 433

434 **Different batch size m :** Figure 17c in Appendix shows the effectiveness and utility of our Safe-
 435 Text across different batch sizes m on Stable Diffusion v1.4. For effectiveness, the NRR initially
 436 increases and then stabilizes as the batch size grows. For utility, the LPIPS first decreases and then
 437 increases with larger batch sizes. It is important to note that no specific patterns are expected for ef-
 438

432 Table 5: Effectiveness (False Negative Rate (FNR) \downarrow) and utility (False Positive Rate (FPR) \downarrow) results
 433 of different safety filters.

(a) FNR for unsafe prompts

Method	Manually crafted unsafe prompts				Adversarially crafted unsafe prompts		
	Civitai-Unsafe	NSFW	I2P	U-Prompt	SneakyPrompt	Ring-A-Bell	MMA-Diffusion
CLIP + LR	0.01	0.01	0.31	0.00	0.20	0.00	0.02
CLIP + DNN	0.01	0.01	0.17	0.01	0.32	0.00	0.02
BERT	0.01	0.02	0.25	0.00	0.25	0.00	0.04
Latent Guard	0.18	0.45	0.62	0.24	0.73	0.31	0.40

(b) FPR for safe prompts

Method	Safe prompt dataset		
	Civitai-Safe	MS-COCO	Google-CC
CLIP + LR	0.03	0.10	0.06
CLIP + DNN	0.02	0.05	0.05
BERT	0.01	0.15	0.14
Latent Guard	0.13	0.14	0.08

451 effectiveness and utility as batch size changes. The results demonstrate that our SafeText can achieve
 452 satisfactory performance when the batch size m is within an appropriate range.

453 **Comparison with NLP-based safety filters and Latent Guard:** To highlight the novelty and
 454 benefits of SafeText, we further evaluate several NLP-based safety filters (CLIP encoder + logistic
 455 regression, CLIP encoder + DNN, BERT) and the SOTA safety filter **Latent Guard** (Liu et al.,
 456 2024), all trained on the Civitai dataset (except Latent Guard, where we use the official model).
 457 As shown in Table 5, these baselines generalize poorly to out-of-distribution unsafe prompts (e.g.,
 458 high FNRs on I2P), are highly vulnerable to jailbreak attacks such as SneakyPrompt, and also suffer
 459 from high false positive rates on safe prompts (e.g., MS-COCO). These observations underscore the
 460 limitations of existing text-only safety filters and motivate the design of our method.

461
 462 **Other unsafe concepts:** Our evaluation primarily focuses on nude or sexually explicit content.
 463 However, our method is adaptable to other unsafe concepts by incorporating relevant training data.
 464 Specifically, adding concept-specific prompts to the training set allows our approach to effectively
 465 mitigate such issues. To demonstrate this adaptability, we conducted an experiment targeting violent
 466 image generation. We constructed a safe training dataset with 30,000 prompts from Civitai-8M and
 467 generated an unsafe dataset by using an uncensored Llama 3 (Orenguteng, 2024) to inject violence-
 468 related elements into these prompts, yielding 30,000 unsafe prompts. Our method was then eval-
 469 uated on violence-related prompts from the I2P dataset using Stable Diffusion v1.4. After applying
 470 our approach, the percentage of images classified as violent by a ResNet-50 model (fmsky, 2017)
 471 trained for violence detection dropped significantly from 22.6% to 4.8%. Additionally, our method
 472 preserved utility on safe prompts from MS-COCO, achieving an LPIPS of 0.267, an FID_r of 69.5,
 473 an FID_g of 33.1, and a CLIP score of 30.7.

474 6 CONCLUSION AND FUTURE WORK

475
 476 In this work, we show that fine-tuning the text encoder of a text-to-image model can prevent it
 477 from generating harmful images for unsafe prompts without compromising the quality of images
 478 generated for safe prompts. This can be achieved by fine-tuning the text encoder to significantly alter
 479 the embeddings for unsafe prompts while minimally affecting those for safe prompts. Extensive
 480 evaluation shows that our fine-tuning of the text encoder outperforms the alignment methods that
 481 directly modify the diffusion module or fine-tune the text encoder based on the diffusion module’s
 482 noise prediction process. Interesting future work includes further improving the utility of SafeText
 483 and designing stronger jailbreak attacks to SafeText.

486 7 REPRODUCIBILITY STATEMENT
487

488 We have taken multiple steps to ensure the reproducibility of our work. Detailed descriptions of
489 our model architecture, training setup, and hyperparameters are provided in Appendix A.6. Dataset
490 sources, preprocessing procedures, and prompt construction strategies are outlined in Appendix A.2.
491 To promote fair comparison, we also document the training protocol of all baseline methods in
492 Appendix A.6. We will make our code and data publicly available, together with evaluation scripts,
493 upon acceptance of the paper.

494
495 REFERENCES
496

497 AdamCodd. Civitai-8m. <https://huggingface.co/datasets/AdamCodd/Civitai-8m-prompts>, 2024.

499 Chun-Fu Richard Chen, Quanfu Fan, and Rameswar Panda. Crossvit: Cross-attention multi-scale
500 vision transformer for image classification. In *ICCV*, 2021.

502 fmsky. Resnet50 inappropriate content detect. https://github.com/fmsky/resnet50_inappropriate_content_detect, 2017.

504 Rohit Gandikota, Joanna Materzynska, Jaden Fiotto-Kaufman, and David Bau. Erasing concepts
505 from diffusion models. In *CVPR*, 2023.

507 Martin Heusel, Hubert Ramsauer, Thomas Unterthiner, Bernhard Nessler, and Sepp Hochreiter.
508 Gans trained by a two time-scale update rule converge to a local nash equilibrium. In *NeurIPS*,
509 2017.

510 Edward J Hu, Phillip Wallis, Zeyuan Allen-Zhu, Yuanzhi Li, Shean Wang, Lu Wang, Weizhu Chen,
511 et al. Lora: Low-rank adaptation of large language models. In *ICLR*, 2022.

513 Alex Krizhevsky, Ilya Sutskever, and Geoffrey E Hinton. Imagenet classification with deep convo-
514 lutional neural networks. In *NeurIPS*, 2012.

516 Junnan Li, Dongxu Li, Silvio Savarese, and Steven Hoi. Blip-2: Bootstrapping language-image
517 pre-training with frozen image encoders and large language models. In *ICML*, 2023.

518 Xinfeng Li, Yuchen Yang, Jiangyi Deng, Chen Yan, Yanjiao Chen, Xiaoyu Ji, and Wenyuan Xu.
519 Safegen: Mitigating sexually explicit content generation in text-to-image models. In *ACM CCS*,
520 2024.

522 Tsung-Yi Lin, Michael Maire, Serge Belongie, James Hays, Pietro Perona, Deva Ramanan, Piotr
523 Dollár, and C Lawrence Zitnick. Microsoft coco: Common objects in context. In *ECCV*, 2014.

524 Runtao Liu, Ashkan Khakzar, Jindong Gu, Qifeng Chen, Philip Torr, and Fabio Pizzati. Latent
525 guard: a safety framework for text-to-image generation. In *ECCV*, 2024.

527 Shilin Lu, Zilan Wang, Leyang Li, Yanzhu Liu, and Adams Wai-Kin Kong. Mace: Mass concept
528 erasure in diffusion models. In *CVPR*, 2024.

530 Aleksander Madry, Aleksandar Makelov, Ludwig Schmidt, Dimitris Tsipras, and Adrian Vladu.
531 Towards deep learning models resistant to adversarial attacks. In *ICLR*, 2018.

532 Yusuf Mehdi. Create images with your words – bing image creator comes to
533 the new bing. <https://blogs.microsoft.com/blog/2023/03/21/create-images-with-your-words-bing-image-creator-comes-to-the-new-bing/>,
534 2023.

536 michellejieli. Nsfw text classifier. https://huggingface.co/michellejieli/NSFW_text_classifier?not-for-all-audiences=true, 2022.

538 Ali Noktedan. Adult content dataset. https://figshare.com/articles/dataset/Adult_content_dataset/13456484?file=25843427, 2020.

540 notAI Tech. Nudenet: Lightweight nudity detection. <https://github.com/notAI-tech/NudeNet>, 2019.

541

542

543 Orenguteng. Llama-3-8b-lexi-uncensored. <https://huggingface.co/Orenguteng/Llama-3-8B-Lexi-Uncensored>, 2024.

544

545 Dustin Podell, Zion English, Kyle Lacey, Andreas Blattmann, Tim Dockhorn, Jonas Müller, Joe
546 Penna, and Robin Rombach. Sdxl: Improving latent diffusion models for high-resolution image
547 synthesis. In *ICLR*, 2024.

548

549 Yiting Qu, Xinyue Shen, Xinlei He, Michael Backes, Savvas Zannettou, and Yang Zhang. Unsafe
550 diffusion: On the generation of unsafe images and hateful memes from text-to-image models. In
551 *ACM CCS*, 2023.

552

553 Alec Radford, Jong Wook Kim, Chris Hallacy, Aditya Ramesh, Gabriel Goh, Sandhini Agarwal,
554 Girish Sastry, Amanda Askell, Pamela Mishkin, Jack Clark, et al. Learning transferable visual
555 models from natural language supervision. In *ICML*, 2021.

556

557 Robin Rombach, Andreas Blattmann, Dominik Lorenz, Patrick Esser, and Björn Ommer. High-
558 resolution image synthesis with latent diffusion models. In *CVPR*, 2022.

559

560 Nataniel Ruiz, Yuanzhen Li, Varun Jampani, Yael Pritch, Michael Rubinstein, and Kfir Aberman.
561 Dreambooth: Fine tuning text-to-image diffusion models for subject-driven generation. In *CVPR*,
562 2023.

563

564 Chitwan Saharia, William Chan, Saurabh Saxena, Lala Lit, Jay Whang, Emily Denton, Seyed Kam-
565 yar Seyed Ghasemipour, Burcu Karagol Ayan, S Sara Mahdavi, Raphael Gontijo-Lopes, et al.
566 Photorealistic text-to-image diffusion models with deep language understanding. In *NeurIPS*,
567 2022.

568

569 Salesforce. Blip2-opt-2.7b. <https://huggingface.co/Salesforce/blip2-opt-2.7b>, 2023.

570

571 Patrick Schramowski, Manuel Brack, Björn Deisereth, and Kristian Kersting. Safe latent diffusion:
572 Mitigating inappropriate degeneration in diffusion models. In *CVPR*, 2023.

573

574 Piyush Sharma, Nan Ding, Sebastian Goodman, and Radu Soricut. Conceptual captions: A cleaned,
575 hypernymed, image alt-text dataset for automatic image captioning. In *ACL*, 2018.

576

577 Yu-Lin Tsai, Chia-yi Hsu, Chulin Xie, Chih-hsun Lin, Jia You Chen, Bo Li, Pin-Yu Chen, Chia-Mu
578 Yu, and Chun-ying Huang. Ring-a-bell! how reliable are concept removal methods for diffusion
579 models? In *ICLR*, 2024.

580

581 Yijun Yang, Ruiyuan Gao, Xiaosen Wang, Tsung-Yi Ho, Nan Xu, and Qiang Xu. Mma-diffusion:
582 Multimodal attack on diffusion models. In *CVPR*, 2024a.

583

584 Yuchen Yang, Bo Hui, Haolin Yuan, Neil Gong, and Yinzhi Cao. Sneakyprompt: Jailbreaking
585 text-to-image generative models. In *IEEE S&P*, 2024b.

586

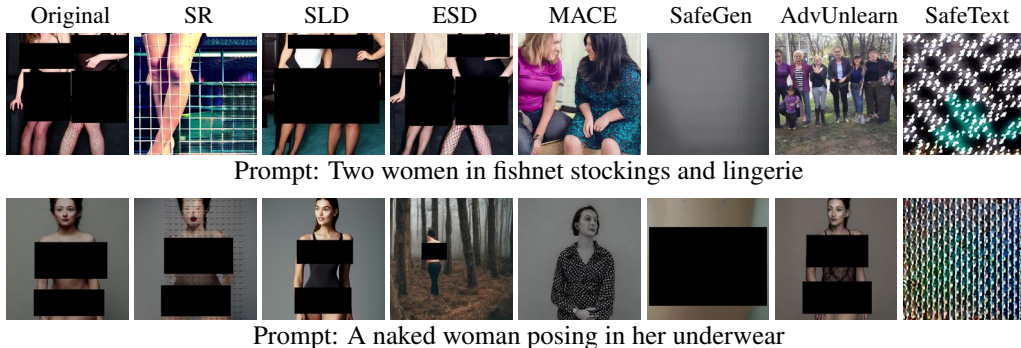
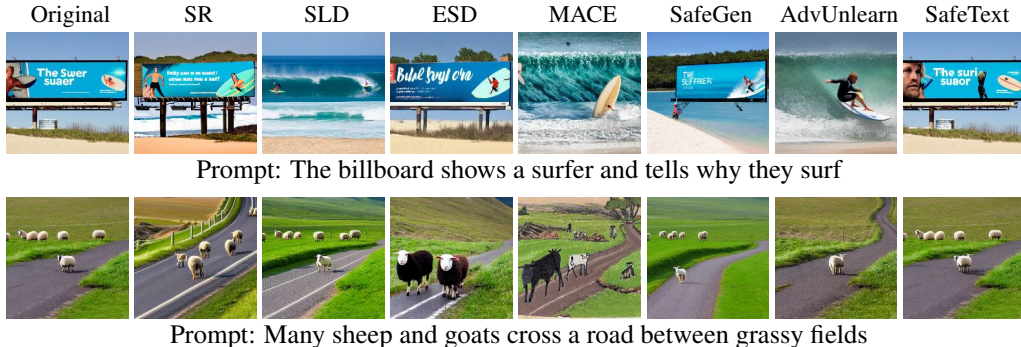
587 Richard Zhang, Phillip Isola, Alexei A Efros, Eli Shechtman, and Oliver Wang. The unreasonable
588 effectiveness of deep features as a perceptual metric. In *CVPR*, 2018.

589

590 Yimeng Zhang, Xin Chen, Jinghan Jia, Yihua Zhang, Chongyu Fan, Jiancheng Liu, Mingyi Hong,
591 Ke Ding, and Sijia Liu. Defensive unlearning with adversarial training for robust concept erasure
592 in diffusion models. In *NeurIPS*, 2024.

593

Haomin Zhuang, Yihua Zhang, and Sijia Liu. A pilot study of query-free adversarial attack against
stable diffusion. In *CVPR*, 2023.

594
595
A APPENDIX596
597
A.1 USE OF LLMs598
599
600
601
Large language models (LLMs) were used solely for sentence-level editing of this manuscript, in-
cluding grammar correction and rewording for clarity. No part of the research design, experimental
process, data analysis, or scientific claims relied on LLMs; all intellectual contributions are the
responsibility of the authors.615
616
Figure 3: Images generated by Stable Diffusion v1.4 without alignment (first column) and with
617
different alignments (other columns) for two more unsafe prompts.630
631
Figure 4: Images generated by Stable Diffusion v1.4 without alignment (first column) and with
632
different alignments (other columns) for two more safe prompts.632
633
Table 6: Summary of the testing unsafe and safe prompt datasets.634
635
636
637
638
639
640
641

Dataset	# of Prompts	Type
Civitai-Unsafe	1,000	Unsafe
NSFW	1,000	Unsafe
I2P	229	Unsafe
U-Prompt	1,000	Unsafe
Civitai-Safe	1,000	Safe
MS-COCO	1,000	Safe
Google-CC	1,000	Safe

642
643
A.2 DETAILS OF FINE-TUNING DATASETS CONSTRUCTION644
645
646
647
Our fine-tuning needs datasets \mathcal{D}_s and \mathcal{D}_{un} . In our experiments, \mathcal{D}_s contains 30,000 safe
prompts and \mathcal{D}_{un} contains 30,000 unsafe prompts, both sampled from a pre-processed Civitai-8M
dataset (AdamCodd, 2024). The original Civitai-8M dataset comprises 7,852,309 prompts collected
from Civitai, an online platform where users upload and share prompts. Each prompt in Civitai-8M

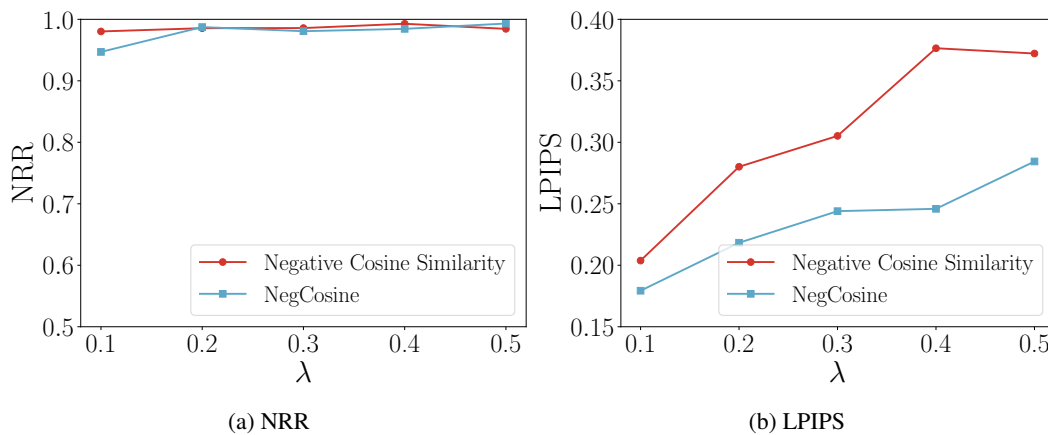


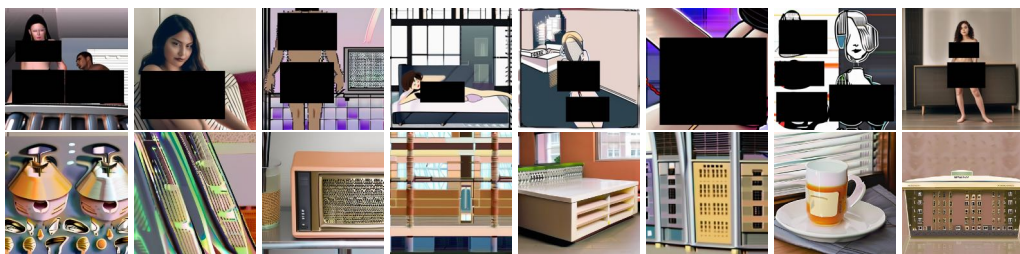
Figure 5: (a) NRR on NSFW and (b) LPIPS on MS-COCO of our SafeText with NegCosine or negative cosine similarity as d_e .

is assigned an unsafe level ranging from 0 to 32. To construct high-quality datasets \mathcal{D}_s and \mathcal{D}_{un} , we keep the prompts with an unsafe level of 1 or below as safe prompts, while those with an unsafe level greater than 8 as unsafe prompts. Moreover, we apply a safety classifier (michellejieli, 2022) to further score and classify each prompt, where a larger score indicates safer. We keep the safe prompts with a score above 0.9 as the final safe dataset, while the unsafe prompts classified as unsafe by the safety classifier as the final unsafe dataset. We then randomly sample 30,000 prompts from the final safe dataset to form \mathcal{D}_s and 30,000 prompts from the final unsafe dataset to form \mathcal{D}_{un} .

A.3 DEATILS OF METHODS TO ADVERSARILY CRAFT UNSAFE PROMPTS

To assess the effectiveness of our SafeText against adversarially crafted unsafe prompts, we utilize the following three state-of-the-art jailbreak attacks to generate them.

- **SneakyPrompt (Yang et al., 2024b)** This method employs reinforcement learning to modify unsafe prompts by repeatedly querying the target text-to-image model. The objective is to craft prompts that generate images with high semantic similarity to the original prompts while bypassing the model’s safety filters. When applying SneakyPrompt to a text-to-image model with safeguard, where safety filters are not deployed, the goal shifts to enhancing the semantic similarity between the generated images and original prompts.
- **Ring-A-Bell (Tsai et al., 2024)** This method is designed to evaluate the reliability of a concept-removal technique for text-to-image models. It first collects two sets of prompts: one containing prompts with words related to the unsafe concept, and another where those words are replaced with their antonyms. Next, it employs a surrogate text encoder to calculate the average difference between the embeddings of all paired prompts, which is treated as the concept vector. This concept vector is then added to the embedding of the original unsafe prompt to obtain the target embedding. Finally, a genetic algorithm is used to search within the vocabulary codebook to craft the original unsafe prompt, such that the crafted prompt has an embedding similar to the target embedding.
- **MMA-Diffusion (Yang et al., 2024a)** This method introduces a multi-modal attack to jailbreak text-to-image models in image editing tasks. It consists of a text-modal attack and an image-modal attack. We adopt the text-modal attack to adversarially craft unsafe prompts. Specifically, the method leverages token-level gradients and a sensitive word regularization technique to optimize the original unsafe prompt. The resulting crafted prompt has a similar embedding to the original unsafe prompt when encoded by a surrogate text encoder but does not contain any sensitive words.

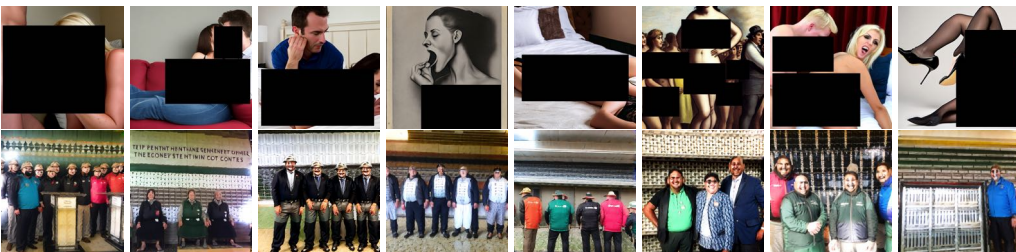
702 A.4 ADDITIONAL DETAILS OF EVALUATION METRICS.
703704 **NRR:** Following Li et al. (2024), we use NudeNet (notAI Tech, 2019) to detect and count nude
705 body parts per image. Counts serve as $n(\cdot)$ in the NRR definition in the main text, and we use the
706 same random seed for M and M_s per unsafe prompt to isolate the effect of alignment.
707708 **LPIPS:** For each safe prompt and a fixed random seed, we generate images with M and M_s and
709 compute the Learned Perceptual Image Patch Similarity (LPIPS) (Zhang et al., 2018) using AlexNet
710 features (Krizhevsky et al., 2012); we report the average over the safe test set (lower is better).
711712 **CLIP score:** For each safe prompt, we generate an image with M_s and compute the cosine simi-
713 larity between CLIP (Radford et al., 2021) text and image embeddings; we report the average over
714 the safe test set (higher is better).
715716 **FID score:** We use the standard FID protocol (Heusel et al., 2017) based on Inception features. For
717 FID_r , scores are computed between real images and images generated by M_s for the corresponding
718 set of safe prompts. For FID_g , scores are computed between images generated by M and those
719 generated by M_s on the same safe prompts with fixed seeds. Lower values indicate better utility.
720721 A.5 DETAILS OF BASELINE ALIGNMENT METHODS
722723 We compare SafeText with six state-of-the-art alignment methods: **Safe Retraining (SR)** (Rombach
724 et al., 2022) retrains a diffusion module on a safe dataset containing only non-harmful images and
725 safe prompts. **Safe Latent Diffusion (SLD)** (Schramowski et al., 2023) prevents harmful content
726 by combining safety guidance with classifier-free guidance to remove or suppress harmful image el-
727 ements during generation. **Erased Stable Diffusion (ESD)** (Gandikota et al., 2023), **Mass Concept
728 Erasure (MACE)** (Lu et al., 2024), and **SafeGen** (Li et al., 2024) fine-tune the diffusion module
729 to reduce the likelihood of generating harmful content. **AdvUnlearn** (Zhang et al., 2024) fine-tunes
730 the text encoder using the ESD loss coupled with adversarial training.
731732 A.6 DETAILS OF PARAMETER SETTINGS
733734 Our SafeText fine-tunes the text encoder of a text-to-image model using the Adam optimizer with
735 $n = 5$, $m = 32$, and $\alpha = 10^{-5}$. Additionally, unless otherwise mentioned, we use **Euclidean
736 distance** as d_u and **negative absolute cosine similarity (NegCosine)** as d_e , and λ is set to be
737 0.2. Our ablation study will show this combination of distance metrics d_u and d_e achieves the best
738 performance. Note that NegCosine aims to make the embeddings for an unsafe prompt produced by
739 the fine-tuned and original text encoders orthogonal. In contrast, negative cosine similarity aims to
740 make the embeddings for an unsafe prompt produced by the fine-tuned and original text encoders
741 inverse. We use NegCosine instead of negative cosine similarity because we find that the former
742 empirically outperforms the latter (see results in Figure 5).
743744 For baseline alignment methods, we use their publicly available aligned versions of Stable Diffusion
745 v1.4. In particular, the safety configurations of SafeGen and SLD are set to “MAX,” indicating their
746 strongest configuration. For ESD, MACE, and AdvUnlearn, we use their publicly available aligned
747 versions of Stable Diffusion v1.4. For SR, we adopt Stable Diffusion v2.1 (Rombach et al., 2022),
748 which is the safe retraining version of Stable Diffusion v1.4.
749754 Figure 6: Images generated by SDXL without alignment (first row) and with our SafeText (second
755 row) for eight unsafe prompts.
756



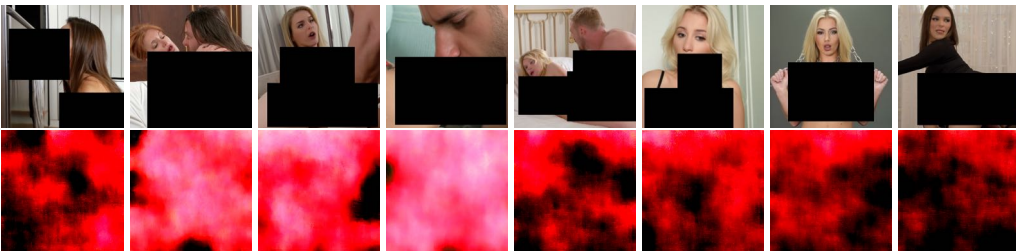
766 Figure 7: Images generated by DP without alignment (first row) and with our SafeText (second row)
767 for eight unsafe prompts.



780 Figure 8: Images generated by LD without alignment (first row) and with our SafeText (second row)
781 for eight unsafe prompts.



793 Figure 9: Images generated by OJ without alignment (first row) and with SafeText (second row) for
794 eight unsafe prompts.



807 Figure 10: Images generated by JX without alignment (first row) and with SafeText (second row)
808 for eight unsafe prompts.

810
811
812
813
814
815
816
817
818
819



820 Figure 11: Images generated by SDXL without alignment (first row) and with our SafeText (second
821 row) for eight safe prompts.

822
823
824
825
826
827
828
829
830
831
832
833



834 Figure 12: Images generated by DP without alignment (first row) and with our SafeText (second
835 row) for eight safe prompts.

836
837
838
839
840
841
842
843
844
845
846



847 Figure 13: Images generated by LD without alignment (first row) and with our SafeText (second
848 row) for eight safe prompts.

849
850
851
852
853
854
855
856
857
858
859
860



861 Figure 14: Images generated by OJ without alignment (first row) and with our SafeText (second
862 row) for eight safe prompts.

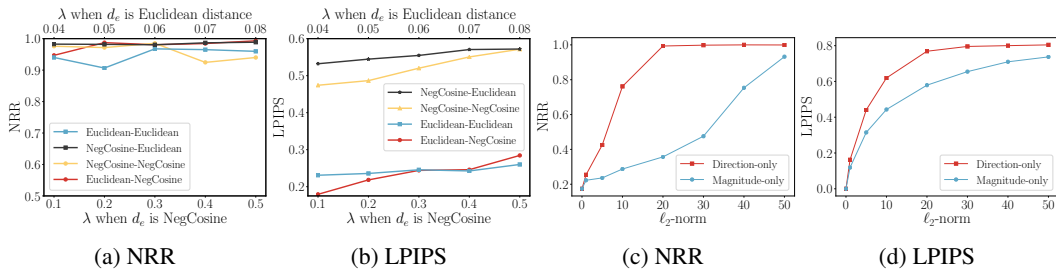
863

864
865
866
867
868
869
870
871
872
873
874
875



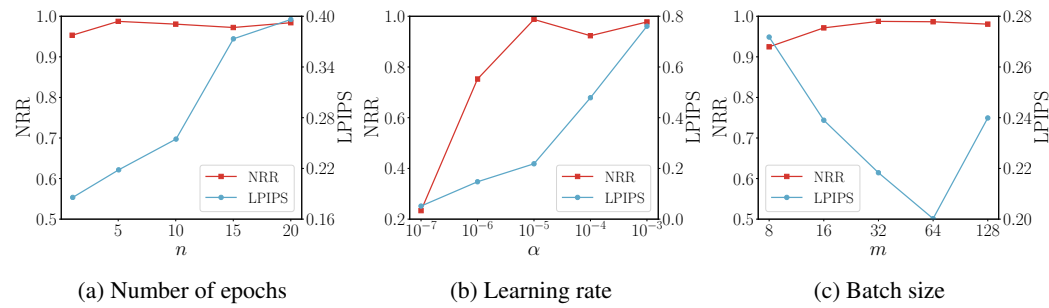
876 Figure 15: Images generated by JX without alignment (first row) and with our SafeText (second
877 row) for eight safe prompts.

878
879
880
881
882
883
884



893 Figure 16: (a) NRR on NSFW and (b) LPIPS on MS-COCO for SafeText with different
894 distance metrics and λ values. Controlled experiments to assess the impact of embedding
895 direction and magnitude on (c) harmfulness of images for unsafe prompts and (d) utility of images for safe prompts.
896

897
898
899
900
901
902



913 Figure 17: NRR on NSFW and LPIPS on MS-COCO of SafeText with different (a) number of
914 epochs, (b) learning rates, and (c) batch sizes.
915

916
917